Quantifying the potential benefits of risk-mitigation strategies on future flood losses in Kathmandu Valley, Nepal

Carlos Mesta[1], Gemma Cremen[2], Carmine Galasso[1,2]

[1]Understanding and Managing Extremes (UME) Graduate School, Scuola Universitaria Superiore (IUSS) Pavia, Pavia, 27100, Italy

[2]Department of Civil, Environmental and Geomatic Engineering, University College London, London, WC1E 6BT J, United Kingdom

Correspondence to: Carmine Galasso (c.galasso@ucl.ac.uk)

Abstract. Flood risk is expected to increase in many regions worldwide due to rapid urbanization and climate change if adequate risk-mitigation (or climate-change-adaptation) measures are not implemented. However, the exact benefits of these measures remain unknown or inadequately quantified for potential future events in some multi-hazard-prone areas such as Kathmandu Valley, Nepal, which this paper addresses. The analysis involves modeling two flood-occurrence cases (with 100-year and 1000-year mean return periods) and using four residential exposure inventories representing the current (2021) urban system or near-future (2031) development trajectories that Kathmandu Valley could experience. The results predict substantial mean absolute financial losses (€ 473 million and € 775 million in repair/reconstruction costs) and mean loss ratios (2.8% and 4.5%) for the respective flood-occurrence cases in current times if the building stock's quality is assumed to have remained the same as in 2011 (Scenario A). Under a "no change" pathway for 2031 (Scenario B), where the vulnerability of the expanding building stock remains the same as in 2011, mean absolute financial losses for the 100-year and 1000-year mean return period flooding occurrences would respectively increase by 16% and 14% over those of Scenario A. However, a minimum (0.20 m) elevation of existing residential buildings located in the floodplains and the implementation of flood-hazard-informed land-use planning for 2031 (Scenario C) could respectively decrease the mean absolute financial losses of the flooding occurrences by 13% and 9%, and the corresponding mean loss ratios by 27% and 23%, relative to those of Scenario A. Moreover, an additional improvement of the building stock's vulnerability that accounts for the multi-hazard-prone nature of the valley (by means of structural retrofitting and building code enforcement) for 2031 (Scenario D) would further decrease the mean loss ratios (respective reductions for the 100-year and 1000-year mean return period flooding occurrences would be 28% and 24% relative to those of Scenario A). The largest mean loss ratios computed in the four scenarios are consistently associated with populations of the highest incomes, which are largely located in the floodplains. In contrast, the most significant benefits of risk mitigation (i.e., largest reduction in mean absolute financial losses or mean loss ratios between scenarios) are experienced by populations of the lowest incomes. This paper's main findings can inform decision makers about the benefits of investing in forward-looking multi-hazard risk-mitigation efforts.

1 Introduction

Flooding is among the world's most prevalent natural hazards (World Meteorological Organization, 2021). Across the world, tens of millions of people are displaced from their homes by flooding each year, while related damage to property and physical infrastructure causes hundreds of billions of U.S. dollars in direct losses (e.g., Hallegatte et al., 2017; IDMC, 2015). For
35 instance, in the United States alone, the national flood-induced average annual losses (AAL) for 2020 were approximately USD 32.1 billion, with the most impoverished communities across the nation experiencing the largest values of this metric normalized on the basis of building replacement cost (Wing et al., 2022). In general, it is estimated that four of every ten people exposed to flood risk globally live in poverty (Rentschler et al., 2022), which means that the human impacts of flooding tend to be concentrated disproportionately among low-income communities and countries. No matter how frequent or small, flood
40 events can disrupt years of development and poverty reduction progress in these countries (Hallegatte et al., 2016).

Moreover, flood risk is expected to increase due to climate change impacts (e.g., intensification of rainfall extremes, sea level rise) and socioeconomic development in flood-prone regions (e.g., Ceola et al., 2014; Hirabayashi et al., 2013; Jongman et al., 2012; Nicholls et al., 2021). Specifically, rapid urbanization – which is expected to mainly feature across cities in Asia and Africa over the next few decades (United Nations, 2019a) – could increase flood exposure and vulnerability (e.g., Hemmati
45 et al., 2020) and intensify flood hazard (by increasing runoff during precipitation events, due to the replacement of natural ground with impermeable surfaces, changes to drainage or irrigation systems, and deforestation, for instance), if not correctly managed. Therefore, there is an urgent need to investigate how cities can effectively adapt to dynamic risk challenges, especially in low-income regions (Cremen et al., 2022b; Fraser et al., 2016; Hinkel et al., 2018; Jongman, 2018).

Nepal is a landlocked country in South Asia, located in the Himalayan region. Its complex topography and social and physical
50 exposure and vulnerability make Nepal particularly susceptible to geological (e.g., earthquakes, landslides) and hydro-meteorological hazards (e.g., floods, droughts). According to the Global Climate Risk Index, Nepal was among the top ten countries most affected by extreme weather events over the 2000-2019 period (Eckstein et al., 2021). Flooding is the most frequent natural hazard affecting Nepal. Apart from fluvial (riverine) flooding during the monsoon season, other types of flooding that the country experiences include pluvial (flash) flooding from heavy rainfall in mountainous areas, glacial lake
55 outburst flooding, and landslide-induced flooding (Landell Mills, 2019). Nepal has a long history of devastating flood events, such as those that occurred in the Eastern region (1987), Central Nepal (1993), and Kushaha (2008) (Adhikari, 2013; Government of Nepal, 2017). Monsoon precipitation across South Asia in August 2017 affected 80% of the Terai region and surrounding districts. The resulting widespread flooding caused 160 deaths and 45 injuries, destroyed 41,626 houses, and partially damaged 150,510 houses. Direct losses were estimated to be USD 584.7 million, of which 32% corresponded to the
60 housing sector (Government of Nepal, 2017).

The 2017 Terai flood and earlier major events have emphasized the significant risk that flooding continuously imposes on the Nepalese population. While flood risk is already substantial, several ongoing trends in the country could further amplify this

risk in the coming years. Firstly, climate change scenarios developed by the Government of Nepal (GoN) (Ministry of Forests and Environment, 2019) reveal a rising trend in precipitation (for all seasons, except the pre-monsoon season) in the medium term (2016-2045) and long-term (2036-2065). Under representative concentration pathways (RCPs) RCP4.5 and RCP8.5 scenarios, average annual precipitation in Nepal is projected to increase by 2.1-7.9% in the medium term and by 6.4-12.1% in the long term. Intense precipitation events for both RCPs would also be more frequent, with the occurrence of "extreme wet" days increasing at higher rates than "very wet" days. Secondly, Nepal is projected to be one of the fastest urbanizing countries in the world over the 2018-2050 period (United Nations, 2019b), which could lead to significantly larger amounts of flood exposure. While urban growth is gaining pace across different regions of Nepal, Kathmandu Valley represents the "hub" of urban development in the country (Timsina et al., 2020). A previous study by the authors (Mesta et al., 2022b) revealed that urban land in Kathmandu Valley could reach 352 km^2 in 2050, almost doubling its current size and covering half the total valley extent. A significant share of this new urbanization is projected to occupy the valley's most hazardous (at least in terms of flooding and liquefaction) and socially-vulnerable regions (Mesta et al., 2022b). Thirdly, other natural hazards such as earthquakes have unveiled the poor state of Nepal's building stock and physical infrastructure, which is caused by a combination of low-quality building materials, deficient construction practices, low compliance with building codes, as well as aging, and deterioration (Bothara et al., 2018; Varum et al., 2018). Traditional materials, such as bamboo/wood, stone, and mud, are still preferred in many regions of the country (especially in rural areas) due to their availability and low cost (Bothara et al., 2018). However, buildings made of bamboo/wood or mud suffer severely from flood damage (e.g., Becker Andrea B. et al., 2011; Fatemi et al., 2020) due to low durability and high permeability. Therefore, it is critical to determine the potential benefits of implementing disaster risk reduction (DRR) strategies in the country (particularly Kathmandu Valley) towards preventing devastating economic losses and casualties in future major natural hazard events.

Over the last few decades, several flood risk assessments have been conducted at various geographic scales, often leveraging the most recent high-resolution flood, assets, and population maps (Rentschler et al., 2022). However, most studies have focused on high-income countries (Chakraborty Jayajit et al., 2014; Oubennaceur et al., 2019), and studies for developing countries have mostly concentrated on large economic centers, such as Jakarta (Budiyono et al., 2015), Dhaka (Gain et al., 2015), or Ho Chin Minh City (Bangalore et al., 2019). Additionally, some researchers have examined how flood adaptation measures (e.g., ring dike, wet-proofing, dry-proofing, elevating roads and buildings) and/or urban development can affect flood risk trajectories (e.g., Chang et al., 2019; de Ruig et al., 2019; de Ruiter et al., 2021; Du et al., 2020; Lasage et al., 2014; Scussolini et al., 2017; Song et al., 2018; Thieken et al., 2016). Similar studies have yet to be conducted for Kathmandu Valley, however.

This study contributes to the efforts required to quantify the benefits of appropriate mitigation strategies on growing flood risk in urban areas for informing and promoting risk-sensitive decision-making (e.g., Cremen et al., 2022; Galasso et al., 2021a). The work explicitly investigates the effect of various risk-mitigation strategies (i.e., elevating buildings, flood-hazard-informed land-use planning, building retrofitting, and building-code enforcement) on flood-induced financial losses in Kathmandu

Valley, Nepal. The methodology integrates a scenario-based flood loss estimation approach, using 100-year and 1000-year mean return period flood occurrence maps and four potential present (2021) and future (2031) exposure and vulnerability scenarios, focusing only on residential buildings. The results can be relevant to various stakeholders, providing a clear quantitative description of the potential flood risk and its mitigation in Kathmandu Valley that can be leveraged for decision-

100   making on investments in risk-reduction programs.

2 Materials and methods

Quantifying flood risk requires modeling hazard (flood extent and flood depths), exposure (locations and characteristics of population and buildings), and vulnerability (the extent to which hazard affects exposed assets). This study focuses on Kathmandu Valley, Nepal, which is surrounded by the Himalayan mountains and lies within the Bagmati river basin. The

105   valley occupies a total area of 721 km^2, extending from 27°49'4" to 27°31'42" latitude and 85°11'19" to 85°33'57" longitude. Kathmandu Valley encloses three districts (Bhaktapur, Kathmandu, and Lalitpur), which comprise five municipal areas and several municipalities and rural municipalities (formerly named village development committees, or VDCs) (Mesta et al., 2022b), Figure 1.
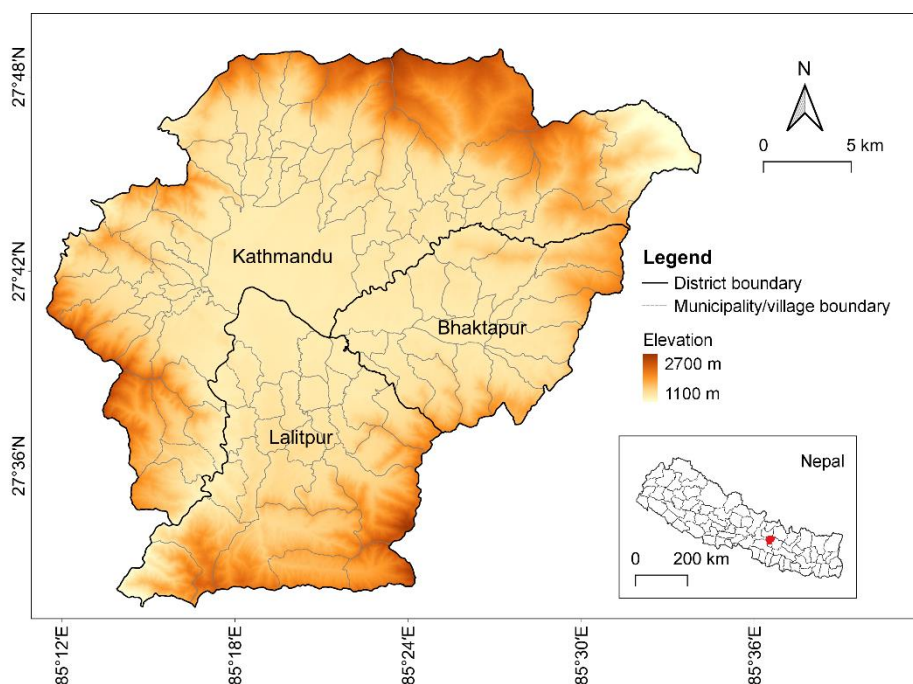
110   **Figure 1.** Physical and administrative map of Kathmandu Valley

2.1 Hazard modeling

We use the high-resolution Fathom-Global model (Sampson et al., 2015), which accounts for both fluvial and pluvial inundation. This global model uses the Multi-Error-Removed Improved-Terrain (MERIT) digital elevation model (Yamazaki et al., 2017) and MERIT Hydro (Yamazaki et al., 2019) as topography and hydrography datasets, respectively. These data

115   provide the most accurate representation of ground surface elevation and location of the rivers at the global scale, which is critical to building robust flood models (Fathom, n.d.). Fluvial inundation is simulated in all river basins with upstream catchment areas larger than 50 km^2. At the same time, pluvial flooding is captured for all catchment sizes by simulating rainfall directly onto the modeled topography. The model considers a 2D shallow-water formulation to explicitly simulate flood wave propagation and a regionalized flood frequency analysis (Smith et al., 2015) to derive river discharge. Fathom-Global provides

120   90 m-resolution maps of flood extents and flood depths for multiple mean return periods (from 1:5 year to 1:1000 year). Note that hazard data of finer resolutions (e.g., 10 m or lower) are recommended for capturing the highly localized nature of flood hazard (e.g., for representing small streams accurately) and associated risks at the urban scale (e.g., Afifi et al., 2019; Nofal and van de Lindt, 2021). In addition, urbanization effects on flood hazard (as a result of increased runoff during rainfall events) are not explicitly accounted for by the Fathom-Global model and are therefore neglected in our analyses. However, the primary

125   purpose of this study is to test different exposure/vulnerability scenarios using a common flood hazard input that is open and easily accessible; developing bespoke fine-resolution flood hazard models for the study area is not within the scope of this work.

We consider two cases of flooding occurrence in Kathmandu Valley. The first case is based on the Fathom-Global undefended flood map with a 100-year mean return period (i.e., 1% annual exceedance probability) and is intended to represent current

130   flood hazard. Decision makers frequently use this type of map (e.g., to identify flood risk zones in the United States). The second flood-occurrence case approximately reflects a situation in which flooding is exacerbated due to climate change and is based on the Fathom-Global undefended flood map with a 1000-year mean return period. The flood maps are resampled to 30 m using the neighbor method to match the spatial resolution of the exposure maps. We combine individual flood maps into aggregated hazard maps that represent fluvial-pluvial flooding for each mean return period by taking their maximum depths

135   in line with the method of Tate et al. (2021). The fluvial-pluvial hazard maps for each considered mean return period are presented in Figure 2. Hereafter, we describe the flooding-occurrence cases using only the terms "100-year" and "1000-year", omitting the description "mean return period" for brevity.
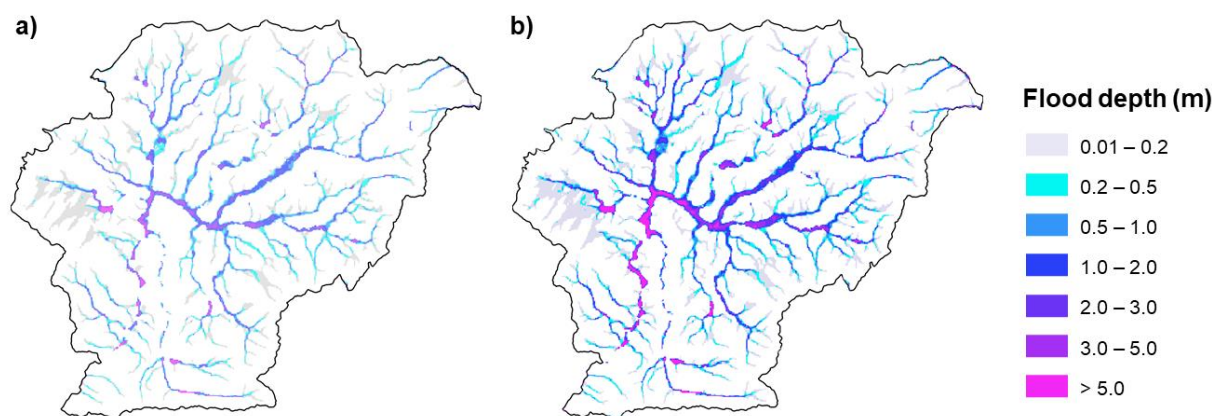
Figure 2. Fluvial-pluvial flood maps for a) 100-year mean return period; and b) 1000-year mean return period flooding occurrences

2.2 Modeling present and future exposure

We use the four exposure scenarios A-D for Kathmandu Valley developed in Mesta et al. (2022a), which are based on the National Population and Housing Census 2011 (Central Bureau of Statistics (CBS), 2012) and various assumptions on the estimated population and number of households for 2021 and 2031. Note that the GoN postponed the census planned for 2021 due to the COVID-19 pandemic, so the characterization of 2021 urban development relies on 10-year-old data.

The proposed scenarios portray different conditions for Kathmandu Valley in terms of urban growth, the prevalence of varying building typologies, and the implementation of DRR measures (see Table 1). Seven building typologies are included in the considered exposure scenarios: adobe (A), brick/stone masonry with mud mortar (BSM), brick/stone masonry with cement mortar (BSC), wood-frame (W), current-construction-practice reinforced concrete (RC-CCP), well-designed reinforced concrete (RC-WDS), and reinforced masonry (RM). These typologies have been previously used by Chaulagain et al. (2016, 2015) as well as Mesta et al. (2022a) to estimate seismic losses in Nepal and Kathmandu Valley. A, BSM, and BSC buildings constitute unreinforced masonry structures. RC-CCP refers to RC frame structures constructed without technical supervision. In contrast, RC-WDS are RC structures with ductile detailing designed according to seismic provisions. RM corresponds to the RM1 (Reinforced Masonry Bearing Walls with Wood or Metal Deck Diaphragms) building typology from the HAZUS Earthquake Model (Federal Emergency Management Agency (FEMA), 2020).

The specifications of each scenario are primarily provided in Mesta et al. (2022a); any deviations in these details for this specific study are documented in Sections 2.2.1 to 2.2.3. Note that we do not consider the presence of basements for any building typology since they do not seem to be a common feature of buildings in the valley (except for a minor proportion of RC buildings). For instance, an extensive post-earthquake damage assessment conducted by the National Society for Earthquake Technology-Nepal (NSET, 2016) described the presence of basements in modern high-rise RC buildings; however,

160 buildings with six or more stories only represent 1% of all buildings in Kathmandu Valley. Suwal et al. (2017) identified the presence of basements in 31% of RC buildings in the valley, but their study was limited to only 64 buildings.

2.2.1 Scenario A (population and buildings for 2021)

In this study, we group the BSM and BSC typologies under an individual building typology, titled BSM/BSC, since using either mud mortar or cement mortar does not alter building flood resistance within the specific vulnerability models used in
165 this study (see Section 2.3). Using the same reasoning, we group RC-CCP and RC-WDS under one building typology labeled RC-CCP/WDS. We determine the proportions of the building typologies per VDC based on the 2011 census data (type of outer wall, type of foundation), as described in Mesta et al. (2022a). The exact height (number of stories) of each building is uncertain and is therefore randomly sampled using typology-specific empirical distributions or single values (not provided in Mesta et al., 2022a) that are derived from data collected for more than 20,000 buildings after the 2015 Gorkha Earthquake by
170 the NSET (2016). These distributions/values are defined as follows: two stories for A and W, between one and four stories (in the respective ratio 0.35:0.40:0.15:0.10) for brick buildings (i.e., BSM, BSC, RM), and between one and five stories (in the respective ratio 0.1:0.1:0.45:0.25:0.1) for concrete buildings (i.e., RC-CCP/WDS).

2.2.2 Scenarios B, C, and D (population and buildings for 2031)

Future exposure for Scenario B is simulated using the proportions of different building typologies and the empirical
175 distributions/values of building heights defined in Scenario A.

Scenario C introduces two DRR measures that can reduce flood risk. The first DRR measure assumes that every existing building in a given floodplain is elevated by 0.2 m, a flood-risk mitigation measure proposed by Du et al. (2020) to reduce flood losses in Shanghai, China. This elevation considers the construction of a 0.2m thick concrete platform above the ground floor, which constitutes a realistic (technically feasible) strategy to potentially reduce flood damage, especially in areas that
180 experience low or moderate flood depths. Greater building elevations (as considered by Du et al., 2020) could prevent larger losses but would reduce household comfort (i.e., result in an excessive decrease in the floor-to-ceiling height). The second DRR measure consists of flood-hazard-informed land-use planning (i.e., the restriction of future urbanization in flood-prone areas). All future buildings are distributed only to the 2031 urban cells outside the corresponding 100-year and 1000-year floodplains. Flooding-informed future urbanization is a reasonable, feasible strategy, as the density of buildings in the selected
185 (non-flooded) 2031 urban cells does not exceed the density of buildings in the existing 2021 urban cells.

Scenario D incorporates DRR measures that account for the multi-hazard-prone nature of Kathmandu Valley and can reduce both flood and seismic risk effectively. This means that it still includes the Scenario D structural retrofitting policies and building code enforcement seismic risk-mitigation interventions introduced in Mesta et al. (2022a) (i.e., A, BSM, BSC building typologies are replaced by RM; the RC-CCP typology is converted to RC-WDS), in addition to the flood-related DRR measures
190 proposed in Scenario C.

2.2.3 Building replacement value

Building replacement value calculations in Mesta et al. (2022a) do not account for variable building heights. Based on the graphical description of buildings provided by Chaulagain et al. (2016) and the data reported by NSET (see Section 2.2.1), we

195 assume that the values of area per building (m^2) included in Chaulagain et al. correspond to two-story buildings for A, W, BSM/BSC, and three-story buildings for RC-CCP/WDS and RC-WDS. This allows us to estimate a ratio of building area per story for each building, subsequently used to derive total costs for buildings with any number of stories. For simplicity, the building area and unit construction cost for the combined BSM/BSC typology (i.e., 75 m^2 and 250 €/m^2) are calculated as the average of the values for both individual typologies reported in Chaulagain et al. (2016). The building area and unit construction cost for the combined RC-CCP/WDS building typology (i.e., 82 m^2 and 318 €/m^2) are computed assuming a 76%-

200 24% contribution of the values for both individual typologies reported in Chaulagain et al. (2016), in line with the relevant proportion of these typologies assumed in Mesta et al. (2022a). The additional costs associated with the elevation of buildings in Scenarios C and D are estimated based on the volume of concrete required to build the elevation platform (which is the platform thickness multiplied by the ratio of building area per story), considering a unit cost of 100 €/m^3 based on expert judgment.

205 **Table 1.** Summary of considered exposure scenarios for Kathmandu Valley

Exposure scenario	Scenario A	Scenario B	Scenario C	Scenario D
Year	2021	2031	2031	2031
Population	3,151,741	3,792,232	3,792,232	3,792,232
Number of buildings	789,898	943,606	943,606	943,606
Aggregated replacement value (€)	17,141,921,300	20,309,544,200	20,380,261,200* 20,409,943,100**	26,442,366,000* 26,470,663,000**
Building typologies featured	A, W, BSM/BSC, RC-CCP/WDS	A, W, BSM/BSC, RC-CCP/WDS	A, W, BSM/BSC, RC-CCP/WDS	RC-WDS, RM
DRR actions	-	-	Elevating buildings, flood-hazard-informed land-use planning	Elevating buildings, flood-hazard-informed land-use planning, structural retrofitting, building code enforcement

Note: Scenarios C and D have two different aggregated replacement values, as the cost of elevating buildings in the 100-year (*) or the 1000-year floodplains (**) differ.

2.3 Modeling flood vulnerability

Since no specific flood vulnerability functions are developed for the study area, we adopt the depth-damage functions of the
210   global flood depth-loss model developed by the Joint Research Center (JRC) of the European Commission (Huizinga et al.,
2017). More sophisticated analytical flood fragility and vulnerability functions, which propagate uncertainties in the hazard-
dependent failure of building components and associated repair/replacement costs (e.g., Nofal et al., 2020; Nofal and van de
Lindt, 2021), would require detailed component-level vulnerability information that is not available for this study.

The JRC vulnerability functions were developed for distinct continents and building occupancies (e.g., residential, commercial,
215   industrial). They express flood depth in meters and losses as mean loss ratios (i.e., financial losses as a percentage of the
building replacement cost). We select the JRC vulnerability function for residential buildings in the Asian continent as our
baseline function. We modify it to consider specific features of Kathmandu Valley's building stock. Firstly, we set a 100%
maximum damage for A and W, and 60% maximum damage for all brick (BSM/BSC, RM) and concrete (i.e., RC-CCP, RC-
WDS) typologies, following JRC recommendations. These damage thresholds are used to scale the loss values of the baseline
220   function and derive two material-specific (i.e., non-resilient and resilient) vulnerability functions. Secondly, we adjust the two
modified material-specific versions of the baseline function to account for different numbers of stories. Since JRC does not
provide relevant information to infer the contribution of different building heights to losses, we assume that the baseline
function is generally representative of two-story buildings and calculate appropriate height-adjustment factors in line with the
procedure introduced in Gentile et al. (2022). These factors are used to multiply the loss values of the two material-specific
225   functions and obtain the six vulnerability functions illustrated in Figure 3. The A building typology is highly vulnerable to
material deterioration from prolonged contact with flood water (e.g., De Risi et al., 2013; Medero et al., 2011; Tiepolo and
Galligari, 2021). The W building typology is also considerably vulnerable to floods (especially high-velocity flows; e.g.,
Becker Andrea B. et al., 2011). Both brick (BSM/BSC, RM) and concrete (i.e., RC-CCP, RC-WDS) typologies have higher
durability compared with A and W, and low permeability and represent the most flood-resistant buildings (e.g., Balasbaneh et
230   al., 2019; Li et al., 2016). Although the flood vulnerability may vary slightly between brick and concrete typologies (e.g.,
URM buildings are less able to resist the pressure of flood water exerted on walls than RM and RC buildings; Englhardt et al.,
2019), these differences are not accounted for in the JRC vulnerability functions and thus are not included in this study.

The height-adjustment procedure of Gentile et al. (2022) assumes that the building replacement value is directly proportional
to the number of stories, which may not be strictly valid (e.g., electrical and mechanical equipment are usually installed on the
235   ground floor and mixed occupancy buildings can have commercial areas on the ground floor, increasing the relative
replacement values of this story). Furthermore, the construction costs considered in this study exclude content costs, such that
the resulting financial losses may be underestimated. However, it should be emphasized that the exact losses for a given
exposure scenario (absolute or relative) are not strictly of interest in this study. Instead, we focus on producing comparable
loss outputs for all exposure scenarios that are based on consistent assumptions. In this way, we aim to investigate how risk
240   changes across the exposure scenarios in a relative sense. It is also worth noting that the uncertainty in the vulnerability model

may strongly affect the loss estimation, particularly in terms of loss variability for a given mean return period. However, such uncertainty may be neglected if mean loss quantities are considered for comparison across different scenarios, as in this study.
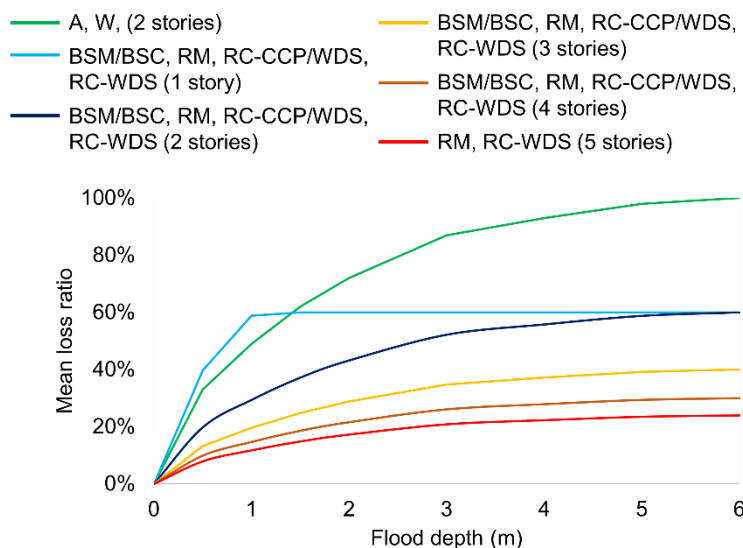
Figure 3. Flood vulnerability functions for the different considered building typologies and their associated range of heights

Moreover, to avoid overestimating losses, we account for the difference between the ground level (above which flood depth is reported in the hazard maps) and the ground-floor level (above which flood depth is measured in the vulnerability functions). We set this difference at 0.2 m, as suggested in previous studies on flooding vulnerability for residential buildings (e.g., Dabbeek et al., 2020; Maqsood et al., 2014; Olsen et al., 2015) and after consulting construction blueprints of buildings in the study area. Furthermore, we use the procedure detailed in Mesta et al. (2022b) to classify populations per VDC as low, middle, or high income for facilitating socioeconomic disaggregation of financial losses.

3 Results and discussion

3.1 Distribution of buildings in the floodplain

Table 2 (rows 1-6) presents a breakdown of the expected number of buildings within various depth ranges of the 100-year floodplain across the four exposure scenarios. In Scenario A, 108,922 buildings (14% of the 2021 building stock) are located in this floodplain, of which 80% and 20% respectively experience flood depths below and above 2.0 m. To provide some context, a 2.0 m flood depth produces mean loss ratios between 43% and 72% for non-elevated buildings with one or two stories and between 17% and 29% for non-elevated buildings with three, four, and five stories. In Scenario B, the larger building stock results in 130,106 buildings positioned within the floodplain (19% more than Scenario A), although the overall proportion of buildings in the floodplain (14% of the 2031 building stock) and their distribution by flood-depth range remains

practically the same as in Scenario A. This means that, considering a 100-year flooding occurrence, future urban expansion (driven by the constraints of past planning decisions) is projected to continue occurring in both inundated and non-inundated areas of the valley. In Scenarios C and D, the expected number of buildings within the floodplain in 2031 remains limited to 2021 levels. Preventing future urbanization in the floodplain decreases the proportion of flood-exposed buildings by 2.2%.

Table 2 (rows 7-12) presents a breakdown of the expected number of buildings within various depth ranges of the 1000-year floodplain across the four exposure scenarios. In Scenario A, 117,179 buildings (15% of the 2021 building stock) are located in this floodplain, of which 66% and 34% respectively experience flood depths below and above 2.0 m. Scenario B results in 180,478 buildings positioned within the floodplain (54% more than Scenario A). In contrast with the 100-year flood-occurrence case, Scenario B shows a notable increase in the total proportion of buildings within the floodplain (19% of the 2031 building stock) relative to Scenario A. This means that, considering a severe flooding occurrence, future expansion (conditioned on past planning decisions) is projected to disproportionately occur in inundated areas. In Scenarios C and D, restricting future urban growth within the floodplain reduces the proportion of flood-exposed buildings by 6.7%.

Table 2. Exposure to flooding: the expected number of buildings in a given range of flood depth per flooding occurrence and exposure scenario. Values in parentheses indicate the proportions of the total building stock represented.

Flooding occurrence	Scenario	0.2-0.5 m	0.5-1.0 m	1.0-2.0 m	2.0-3.0 m	3.0-5.0 m	>5-0 m
100-year	A	29,672	27,308	30,220	13,697	7,118	907
		(3.8%)	(3.5%)	(3.8%)	(1.7%)	(0.9%)	(0.1%)
	B	36,103	31,897	34,973	16,177	9,319	1,636
		(3.8%)	(3.4%)	(3.7%)	(1.7%)	(1.0%)	(0.2%)
	C, D	29,672	27,308	30,220	13,697	7,118	907
		(3.1%)	(2.9%)	(3.2%)	(1.5%)	(0.8%)	(0.1%)
1000-year	A	25,677	22,987	28,899	16,314	17,154	6,194
		(3.3%)	(2.9%)	(3.7%)	(2.1%)	(2.2%)	(0.8%)
	B	40,281	33,095	42,170	22,951	27,330	14,649
		(4.3%)	(3.5%)	(4.5%)	(2.4%)	(2.9%)	(1.6%)
	C, D	25,677	22,987	28,899	16,314	17,154	6,194
		(2.7%)	(2.4%)	(3.1%)	(1.7%)	(1.8%)	(0.7%)

Figure 4 presents additional VDC-level insights on the spatial distribution of buildings within the 100-year floodplain. We identify a large variability in the percentage of buildings in inundated areas and the prevalence of different flood depths across the valley. For Scenario A, proportions of buildings within the floodplain are equal to or less than 10% for 56 VDCs, between 10% and 20% for 40 VDCs, and between 20% and 24% for 8 VDCs. Most VDCs with the largest proportions of buildings in inundated areas are located around the central and northern parts of the valley. Scenario B reflects the effects of not controlling future urbanization in flood-prone areas; proportions of buildings within the floodplain are equal to or less than 10% for only

44 VDCs, between 10% and 20% for 50 VDCs, and between 20% and 30% for 10 VDCs. In contrast, the proportions of buildings within the floodplain for Scenarios C and D are equal to or less than 10% for 79 VDCs, between 10% and 20% for 22 VDCs, and between 20% and 21% for 3 VDCs, reflecting the benefits of constraining future urbanization to non-inundated areas.

285 Figure 5 presents the VDC-level spatial distribution of buildings within the 1000-year floodplain. For Scenario A, proportions of buildings within the floodplain are equal to or less than 10% for 49 VDCs, between 10% and 20% for 43 VDCs, and between 20% and 28% for 12 VDCs. Corresponding Scenario B proportions are equal to or less than 10% for 31 VDCs, between 10% and 20% for 50 VDCs, and between 20% and 40% for 23 VDCs. Corresponding proportions for Scenarios C and D are equal to or less than 10% for 75 VDCs, between 10% and 20% for 24 VDCs, and between 20% and 25% for 5 VDCs.

290
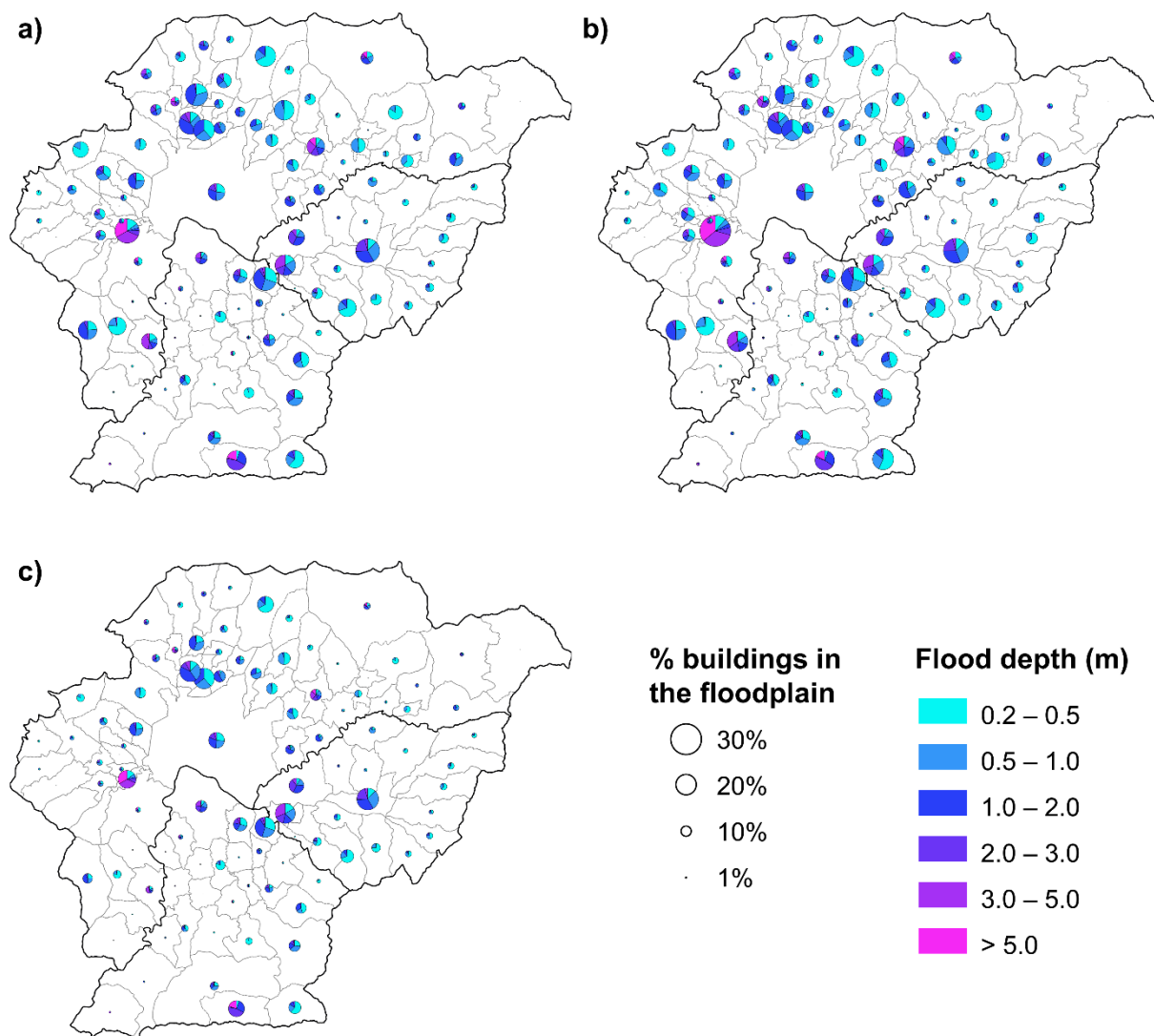
Figure 4. Spatial distribution of buildings in the 100-year floodplain for a) Scenario A, b) Scenario B, and c) Scenarios C and D
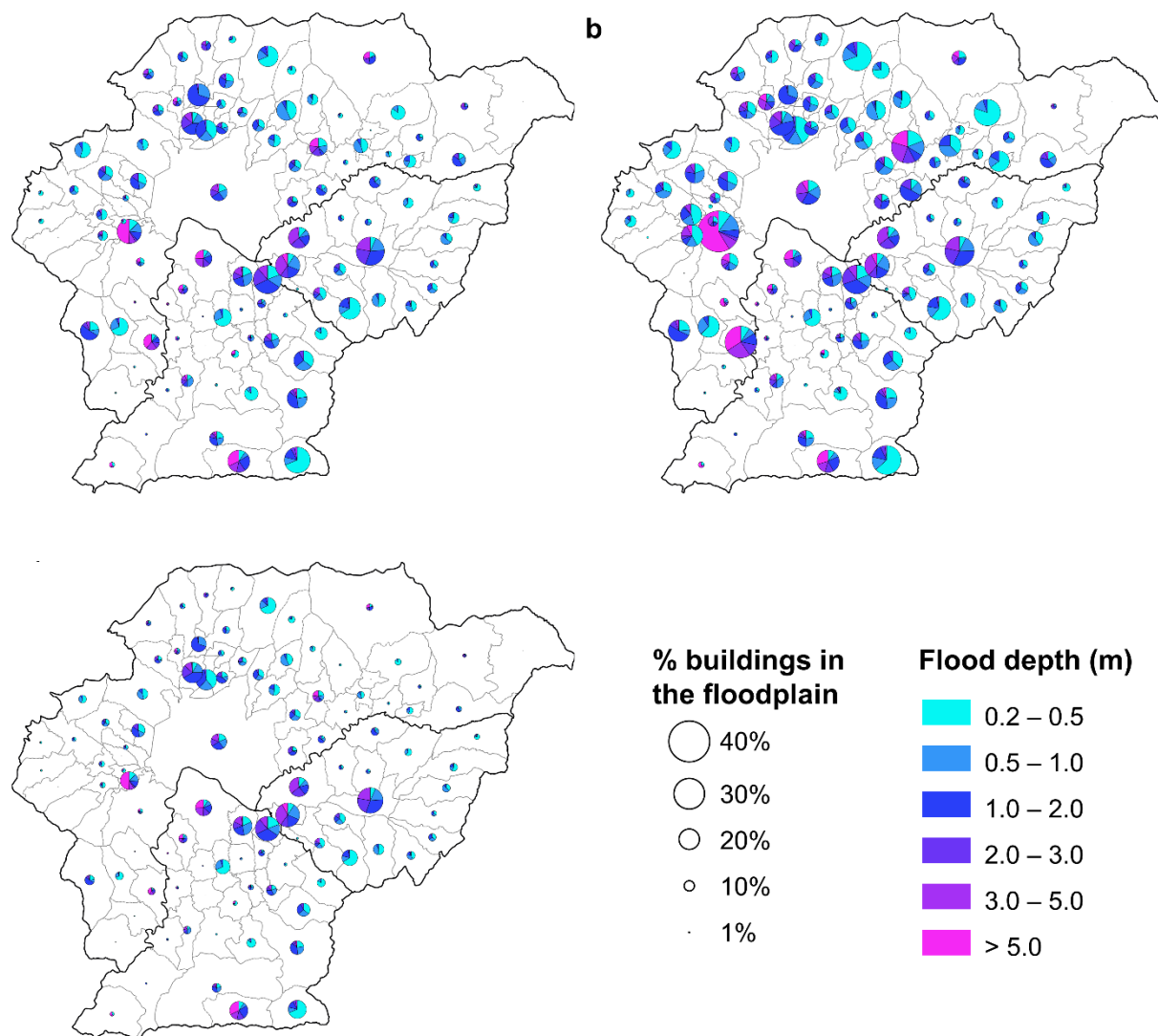
Figure 5. Spatial distribution of buildings in the 1000-year floodplain for a) Scenario A, b) Scenario B, and c) Scenarios C and D

295

3.2 Losses

300 Figure 6 (panels a, b) presents the mean loss ratios associated with the 100-year flooding occurrence, disaggregated by district and income level. From panel a, we observe some variability in the mean loss ratios by district. The Bhaktapur district exhibits the largest mean loss ratios for all the scenarios, which is explained by its disproportionate share of exposure in inundated areas (there are only minor differences in the prevalence of different building typologies between districts, and the three districts are dominated by brick and concrete building typologies that are assumed to have the same level of flood vulnerability;

305 see Section 2.3.) For instance, in Scenario A, the percentage of buildings in the floodplain is 14.9% in Bhaktapur, 14.5% in Kathmandu, and only 9.8% in Lalitpur. Proportions of buildings that experience flood depths below and above 2.0 m respectively are 72%-28% in Bhaktapur, 84%-16% in Kathmandu, and 66%-34% in Lalitpur. Similar results are observed for Scenario B, because the overall proportion of buildings within different flood-depth ranges of the floodplain remains largely identical (see Table 2), and the building stock's vulnerability is not changed. While DRR measures implemented in Scenarios

310 C and D reduce the mean loss ratios compared with those of Scenario B, the relative differences in mean loss ratios between districts are not particularly affected.

From Figure 6 (panel b), we identify some variability in the mean loss ratios by income level. All scenarios produce the highest mean loss ratios for the high-income population, which reflects their disproportionate share of buildings in inundated areas (there are also minor differences in the prevalence of building typologies between income groups, but the three income groups

315 are dominated by brick and concrete typologies). For instance, in Scenario A, the proportion of buildings in the floodplain is 15% in high-income VDCs, 11% in middle-income VDCs, and 12% in low-income VDCs. Proportions of buildings that experience flood depths below and above 2.0 m, respectively, are 81%-19% for high-income VDCs, 75%-25% for middle-income VDCs, and 84%-16% for low-income VDCs. Scenario B shows similar results to Scenario A due to its similar proportions of buildings within different flood-depth ranges of the floodplain (see Table 2) and its identical quality of building

320 stock. In addition, the benefits that result from the building elevation strategy and flood-hazard-informed land-use planning proposed in Scenario C are larger for the low-income population than for the other income groups; the mean loss ratio decreases from Scenario B to C by 44% for the low-income VDCs, by 28% for the middle-income VDCs, and by 22% for the high-income VDCs. There are two main reasons for this trend. On the one hand, low-income VDCs contain the largest proportion of flood-exposed buildings in areas with flood depths below 1.0 m, where the effects of the elevation strategy are more

325 noticeable (as implied by the steep initial slopes of the vulnerability curves presented in Figure 3). In Scenario B, the proportion of buildings that experience flood depths below 1.0 m is 63% for low-income VDCs, 50% for middle-income VDCs, and 51% for high-income VDCs. On the other hand, the proportions of new Scenario B buildings located in the floodplain are higher across low-income VDCs (34% in total) than across middle-income (24%) and high-income (11%) VDCs. Furthermore, the benefits from the multi-hazard (i.e., flooding and seismic) risk-mitigation measures integrated within Scenario D are slightly

330 better than those from the single-hazard-focused Scenario C: between Scenarios B and D, the mean loss ratio drops by 45% for the low-income VDCs, by 29% for the middle-income VDCs, and by 23% for the high-income VDCs.

Figure 6 (panels c, d) presents the mean loss ratios associated with the 1000-year flooding occurrence, disaggregated by district and income level. Similar to the 100-year flood case, there is an implicit relationship between the mean loss ratios and the extent of exposure in inundated regions; the same general trends for mean loss ratio across districts and income levels are
335   observed for the more severe flooding occurrence. Bhaktapur district exhibits the highest mean loss ratios for all exposure scenarios, followed by Kathmandu and Lalitpur. All exposure scenarios result in the highest mean loss ratios for the high-income population, followed by the middle-income and low-income populations. The largest benefits from the risk mitigation strategies are also associated with the low-income population.
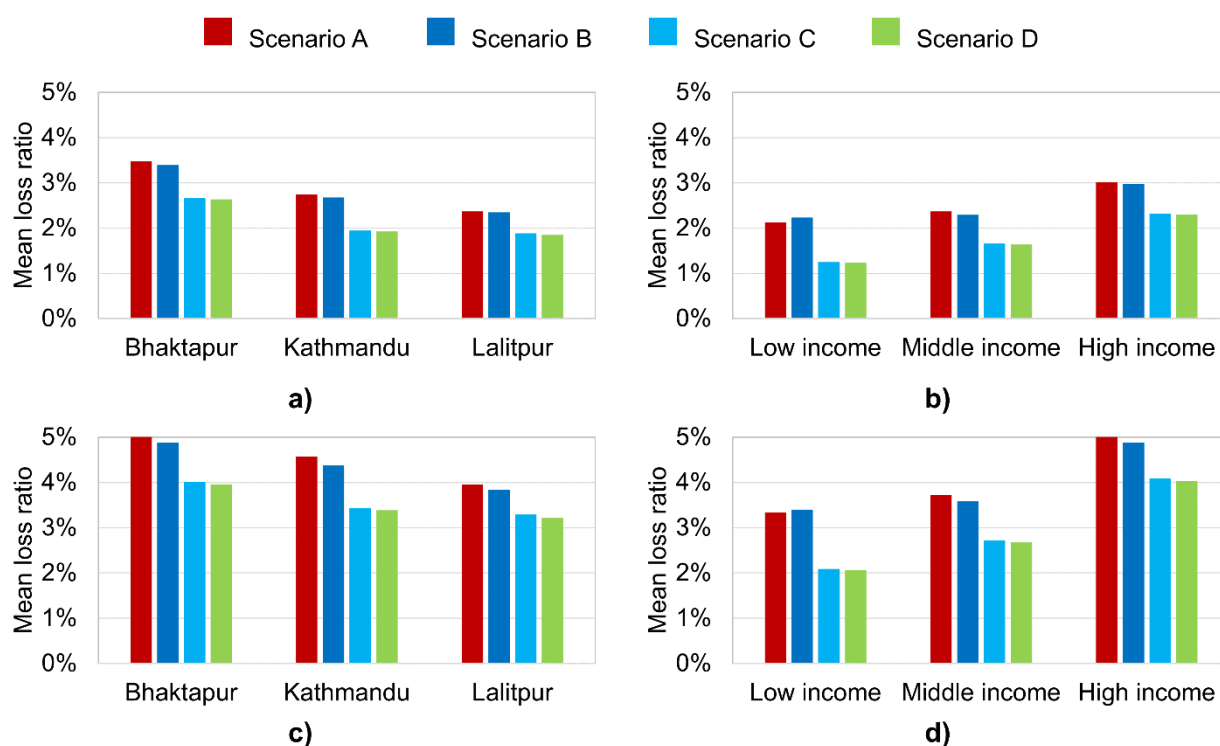
Figure 6. Mean loss ratios disaggregated by district (panels a, c) and income level (b, d), corresponding to the 100-year (upper panels) and 1000-year (lower panels) flooding occurrences

Table 3 summarizes the changes in mean loss ratios and mean absolute financial losses (i.e., repair/reconstruction costs) for both flooding occurrences, considering Scenario A as a baseline. These results reveal how "no action" and implementing DRR measures could affect flood risk in Kathmandu Valley. In the 2021 exposure scenario, 3,151,741 people live in 789,898
345   buildings, with a total replacement value of € 17.1 billion. The 100-year mean absolute financial losses estimated for Scenario A are almost € 473 million (corresponding to a mean loss ratio of 2.8%), while the mean absolute financial losses for the more severe 1000-year flooding occurrence are nearly € 775 million (corresponding to a mean loss ratio of 4.5%).

In the 2031 exposure scenarios, 3,792,232 people are allocated across 524 943,606 buildings, which have a total replacement value of € 20.3 billion in Scenario B, € 20.4 billion in Scenario C, and € 26.4 billion in Scenario D. Changes to mean absolute

350 financial losses associated with the 100-year flooding occurrence and the 2031 exposure scenarios are as follows: they increase by more than € 74 million (+16%) in Scenario B, decrease by more than € 63 million (-13%) in Scenario C, and rise by more than €52 million in Scenario D (+11%), relative to Scenario A. For the 1000-year flooding occurrence, mean absolute losses increase by nearly € 108 million (+14%) in Scenario B, decrease by more than € 66 million (-9%) in Scenario C, and rise by more than € 130 million in Scenario D (+17%), relative to Scenario A. The relative increase in mean absolute financial losses

355 for Scenario B is due to the presence of more assets in the floodplain. In other words, Scenario B demonstrates that a larger population can easily lead to greater flood losses when risk mitigation is neglected. In contrast, the relative decrease in mean absolute financial losses for Scenario C shows that, despite a growing population, elevating existing buildings and implementing flood-hazard-informed land-use planning could significantly reduce flood losses in the future. However, it should be noted that risk-mitigation actions implemented in Scenario C would still leave the building stock highly vulnerable

360 to earthquakes, and thus do not completely address multi-hazard risk in the valley, which is left to Scenario D. The relative increase in mean absolute financial losses in Scenario D is associated with the larger replacement value of its building stock (due to the structural retrofitting and building code enforcement measures implemented), highlighting a tension between short-term (pre-hazard occurrence) costs and long-term benefits (i.e., after the occurrence of hazard events) associated with holistic DRR measures. In summary, Scenario D demonstrates that, despite a growing population, adequate DRR measures that aim

365 to improve the building stock's quality (for better sustaining both flood and earthquake damage) as well as incentivize urbanization away from flood-sensitive areas can limit (but not reduce) flood losses in the future.

Changes to the mean loss ratios provide additional interesting findings. In Scenario A, the mean loss ratios associated with the 100-year and 1000-year flooding occurrences are 2.8% and 4.5%, respectively. In Scenario B, as future urbanization continues occurring in both inundated and non-inundated areas and there are no changes in the building stock's quality, the mean loss

370 ratios only show minimum variations compared to Scenario A. In Scenario C, elevating buildings and the promotion of flood-hazard-informed land use produce a significant decrease in the mean loss ratios, which drop to 2.01% and 3.5% (27% and 23% smaller than in Scenario A), respectively. Due to additional improvements in the building stock's quality in Scenario D, the mean loss ratios drop further to 1.99% and 3.4% (28% and 24% smaller than in Scenario A, respectively). By comparing the mean loss ratios from both Scenarios C and D relative to Scenario A, we notice that seismic-risk mitigation interventions by

375 themselves do not contribute much to reducing flood risk in the valley due to the low replacement rate (<5%) of non-flood-resilient buildings (i.e., A, W) with flood-resilient buildings (i.e., RM) as a result of the seismic upgrading process. However, it is important to remember that Scenario D represents a much more robust approach to multi-hazard risk mitigation than Scenario C.

380

Table 3. Mean loss metrics for Scenario A, and changes to these metrics in Scenarios B, C, and D

Flooding occurrence	Metric		Scenario A	Scenario B	Scenario C	Scenario D
100-year	Mean absolute financial losses (€)		472,932,965	+ 74,654,044	-63,283,799	+ 52,691,045
	Mean loss ratio		2.8%	-0.06%	-0.75%	-0.77%
1000-year	Mean absolute financial losses (€)		774,793,163	+ 107,901,808	-66,393,767	+ 130,500,162
	Mean loss ratio		4.5%	-0.17%	-1.0%	-1.1%

Figure 7 presents additional insights on the VDC-level spatial distribution of the mean loss ratio for the 100-year flooding occurrence. The alignment between the proportion of buildings located in inundated areas and the mean loss ratios is clear when the maps from Figure 7 and Figure 4 are compared; many VDCs with the largest mean loss ratios are situated in or around the central part of the valley. However, VDCs with notable mean loss ratios are not always associated with the largest proportions of buildings in inundated areas; some are simply subjected to relatively high flood depths. Nevertheless, the relative effects of the building elevation strategy and the flood-hazard-informed land-use planning proposed in Scenario C are noticeable: mean loss ratios decrease in five VDCs by 2.0-4.2%, in 27 VDCs by 1.0-2.0%, in 36 VDCs by 0.5-1.0%, and in 36 VDCs by 0%-0.5%, relative to Scenario A (or B). The benefits of implementing additional multi-hazard DRR measures in Scenario D are quite similar to those in Scenario C: mean loss ratios decrease in five VDCs by 2.0-4.2%, in 28 VDCs by 1.0-2.0%, in 35 VDCs by 0.5-1.0%, and in 36 VDCs by 0%-0.5%, relative to Scenario A (or B). Similar observations can be made regarding the VDC-level spatial distribution of the mean loss ratio for the 1000-year flooding occurrence, depicted in Figure 8. The effects of the flood-specific DRR measures implemented in Scenario D are as follows: mean loss ratios decrease in 12 VDCs by 2.0-7.8%, in 36 VDCs by 1.0-2.0%, in 33 VDCs by 0.5-1.0%, and in 22 VDCs by 0%-0.5%, relative to Scenario A or B. The benefits of the combined DRR measures in Scenario D are the following: mean loss ratios decrease in 13 VDCs by 2.0-7.9%, in 35 VDCs by 1.0-2.0%, in 35 VDCs by 0.5-1.0%, and in 20 VDCs by 0%-0.5%, relative to Scenario A or B.
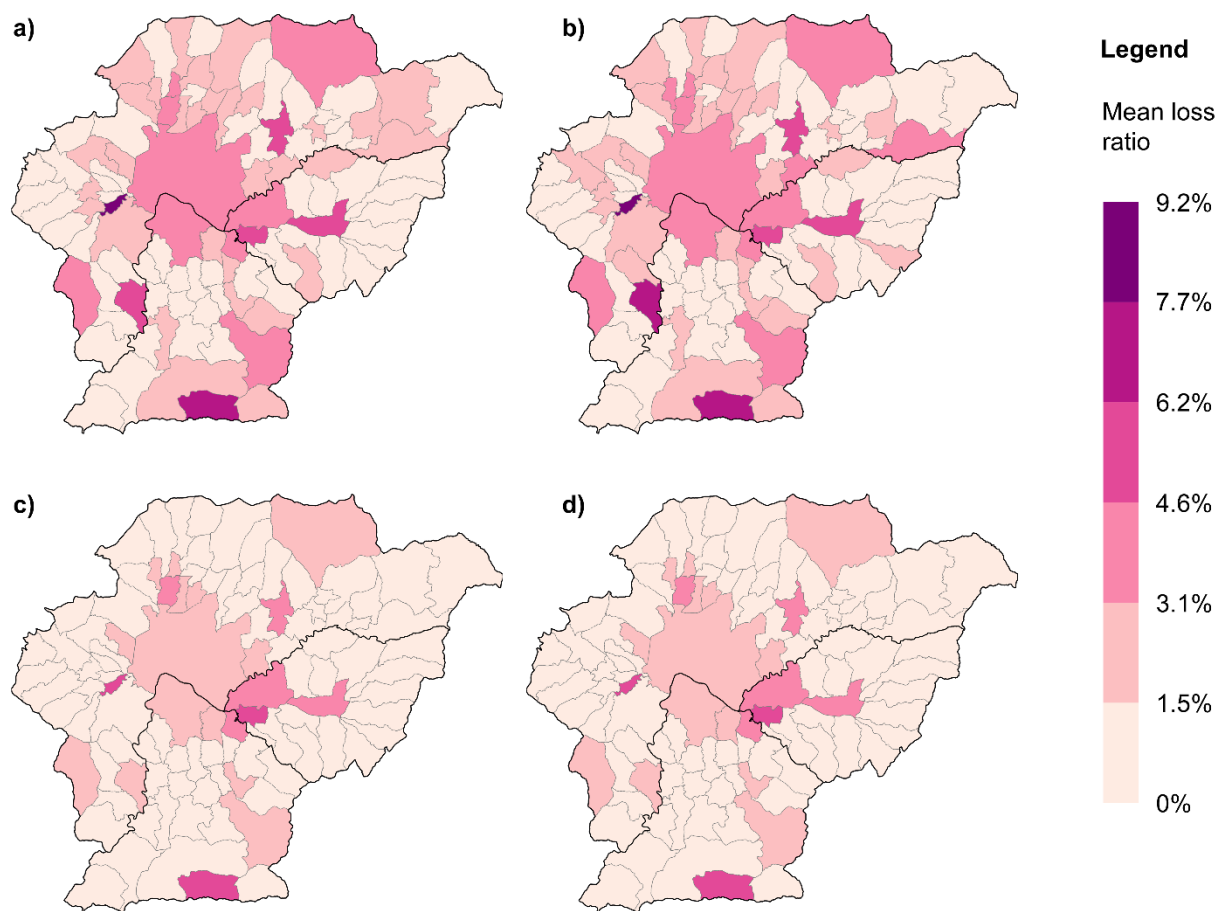
Figure 7. Spatial distribution of mean loss ratios, associated with the 100-year flooding occurrence, for a) Scenario A; b) Scenario B; c)
400   Scenario C; and d) Scenario D

Figure 8. Spatial distribution of mean loss ratios, associated with the 1000-year flooding occurrence, for a) Scenario A; b) Scenario B; c) Scenario C; and d) Scenario D

4 Conclusions

This study has examined the present (2021) and future (2031) flood risk in Kathmandu Valley, considering 100-year and 1000-year mean return period flooding occurrences. Different assumptions on the estimated population, number of households, and building stock quality have been made to construct four plausible current and near-future urban development states for the valley.

Results reveal that a significant proportion of the current building stock is located within the 100-year and 1000-year floodplains (14% and 15%, respectively), which may lead to significant losses. However, an appropriate combination of DRR measures (i.e., building elevation and flood-hazard-informed land-use planning) can substantially limit mean absolute financial losses and reduce relative versions of these losses (i.e., expressed as a proportion of associated replacement costs) in the future,

compared to equivalent current levels. This study reveals that high-income populations are exposed to the highest mean loss ratios across both flooding-occurrence cases due to having the largest proportions of buildings in the floodplain. This contrasts with the trend in income versus earthquake-related losses identified for the same region in previous work (Mesta et al., 2022a), where low-income populations exhibited the highest seismic risk. This discrepancy illustrates that risk-mitigation measures

420 can have varying effects for different hazards; therefore, DRR plans should be appropriately tailored for a specific region or sub-region and account for multiple hazards. Kathmandu Valley's building stock is highly vulnerable to earthquakes due to the prevalence of URM buildings (particularly in low-income VDCs), such as adobe and brick/stone masonry. However, this feature of the building stock does not make it particularly susceptible to flood damage (except in the case of adobe houses, which are made of mud), which is why a multi-hazard approach to DRR that also considers earthquake vulnerability

425 strengthening measures has little effect on the mean loss ratios (and even results in increased mean absolute financial losses) in this study. Instead, the flood risk is mainly controlled by the extent to which populations are located in the floodplain. Considering that hazard intensities vary spatially and that flooding and earthquake-induced ground shaking can affect different proportions of buildings in a given VDC, combinations of individual DRR measures should be investigated to find the optimal DRR solution for a given VDC. Furthermore, this study demonstrates that DRR initiatives uniformly targeting flood risk across

430 different income levels produce the largest benefits for low-income populations. These findings are relevant because the benefits of mitigation measures are currently not well understood/quantified by various stakeholders in Nepal.

While this paper is focused on two levels of flooding occurrence, future research could analyze further scenarios to provide more robust results. Nonetheless, we do not expect the general trends identified in this study to significantly differ for other flood occurrence cases. Fine-resolution local hazard models (if and when available) could be used to more accurately quantify

435 flood hazard (and the associated risk), explicitly including the effect of building footprints, climate change, etc. Moreover, updated census information (when available) could be employed to adjust present and future exposure estimations. In addition, the accuracy of the characterization of physical vulnerability could be improved through appropriate modifications to the selected vulnerability functions in line with local construction practices. Future research could also investigate the effectiveness of other possible flood-related DRR actions (e.g., ring dike, wet-proofing, dry-proofing, nature-based solutions, relocation).

440 Lastly, while the benefits of risk-mitigation plans have been discussed in this paper without a proper analysis of costs, various methods such as cost-benefit evaluations (e.g., de Ruig et al., 2019; Du et al., 2020; Gentile and Galasso, 2021; Lasage et al., 2014; Scussolini et al., 2017) or multi-criteria decision making (e.g., Ahmadisharaf et al., 2016; Cremen et al., 2022a; Ruangpan et al., 2021), can help in selecting optimal risk-mitigation solutions.

In summary, this paper addresses the essential need to communicate the growing flood risk in Kathmandu Valley and

445 potentially encourage local (or even Nepal-wide) risk-mitigation efforts. The adopted methodology can be easily extended to other geographical contexts to quantify the impacts of other (multiple) natural hazards on the present and future built environment, providing decision makers with an adequate understanding of the risk consequences of particular actions and the importance of particular risk mitigation/adaptation strategies (Cremen et al., 2022b; Galasso et al., 2021).

450 *Data availability.* The datasets used and/or analyzed during the current study are available from the corresponding author on
reasonable request.

Author contributions. C.M., G.C., and C.G. conceived and designed the research. C.M. drafted the written content of the
manuscript, performed the calculations, and developed the figures. All authors reviewed the manuscript.

455

Competing interests. The authors declare no competing interests.

Acknowledgments. Carlos Mesta was supported by a Research Scholarship from the European Centre for Training and
Research in Earthquake Engineering (EUCENTRE). Carmine Galasso and Gemma Cremen acknowledge funding from UKRI
460 GCRF under grant NE/S009000/1, Tomorrow's Cities Hub.

References

Adhikari, R.: Flooding and Inundation in Nepal Terai: Issues and Concerns, Hydro Nepal, 2013.

Afifi, Z., Chu, H.-J., Kuo, Y.-L., Hsu, Y.-C., Wong, H.-K., and Zeeshan Ali, M.: Residential Flood Loss Assessment and Risk
Mapping from High-Resolution Simulation, Water, 11, 2019.

465 Ahmadisharaf, E., Kalyanapu, A. J., and Chung, E.-S.: Spatial probabilistic multi-criteria decision making for assessment of
flood management alternatives, J. Hydrol., 533, 365–378, 2016.

Balasbaneh, A. T., Bin Marsono, A. K., and Gohari, A.: Sustainable materials selection based on flood damage assessment for
a building using LCA and LCC, J. Clean. Prod., 222, 844–855, 2019.

Bangalore, M., Smith, A., and Veldkamp, T.: Exposure to Floods, Climate Change, and Poverty in Vietnam, Econ. Disasters
470 Clim. Change, 3, 79–99, 2019.

Becker, A., Johnstone, W., and Lence, B.: Wood Frame Building Response to Rapid-Onset Flooding, Nat. Hazards Rev., 12,
85–95, 2011.

Bothara, J., Ingham, J., and Dizhur, D.: Chapter 11 - Earthquake Risk Reduction Efforts in Nepal, in: Integrating Disaster
Science and Management, edited by: Samui, P., Kim, D., and Ghosh, C., Elsevier, 177–203, 2018.

475 Budiyono, Y., Aerts, J., Brinkman, J., Marfai, M. A., and Ward, P.: Flood risk assessment for delta mega-cities: a case study
of Jakarta, Nat. Hazards, 75, 389–413, 2015.

Central Bureau of Statistics (CBS): National Population and Housing Census 2011, Government of Nepal, National Planning Commission Secretariat, Kathmandu, Nepal, 2012.

480 Ceola, S., Laio, F., and Montanari, A.: Satellite nighttime lights reveal increasing human exposure to floods worldwide, Geophys. Res. Lett., 41, 7184–7190, 2014.

Chakraborty Jayajit, Collins Timothy W., Montgomery Marilyn C., and Grineski Sara E.: Social and Spatial Inequities in Exposure to Flood Risk in Miami, Florida, Nat. Hazards Rev., 15, 04014006, 2014.

Chang, S. E., Yip, J. Z. K., and Tse, W.: Effects of urban development on future multi-hazard risk: the case of Vancouver, Canada, Nat. Hazards, 98, 251–265, 2019.

485 Chaulagain, H., Rodrigues, H., Silva, V., Spacone, E., and Varum, H.: Seismic risk assessment and hazard mapping in Nepal, Nat. Hazards, 78, 583–602, 2015.

Chaulagain, H., Rodrigues, H., Silva, V., Spacone, E., and Varum, H.: Earthquake loss estimation for the Kathmandu Valley, Bull. Earthq. Eng., 14, 59–88, 2016.

Cremen, G., Galasso, C., and McCloskey, J.: A Simulation-Based Framework for Earthquake Risk-Informed and People-490 Centered Decision Making on Future Urban Planning, Earths Future, 10, e2021EF002388, 2022a.

Cremen, G., Galasso, C., and McCloskey, J.: Modelling and Quantifying Tomorrow's Risks from Natural Hazards, Sci. Total Environ., 2022b.

Dabbeek, J., Silva, V., Galasso, C., and Smith, A.: Probabilistic earthquake and flood loss assessment in the Middle East, Int. J. Disaster Risk Reduct., 49, 101662, 2020.

495 De Risi, R., Jalayer, F., De Paola, F., Iervolino, I., Giugni, M., Topa, M. E., Mbuya, E., Kyessi, A., Manfredi, G., and Gasparini, P.: Flood risk assessment for informal settlements, Nat. Hazards, 69, 1003–1032, 2013.

Du, S., Scussolini, P., Ward, P. J., Zhang, M., Wen, J., Wang, L., Koks, E., Diaz-Loaiza, A., Gao, J., Ke, Q., and Aerts, J. C. J. H.: Hard or soft flood adaptation? Advantages of a hybrid strategy for Shanghai, Glob. Environ. Change, 61, 102037, 2020.

Eckstein, D., Hutfils, M.-L., and Winges, M.: Global Climate Risk Index 2021, Germanwatch e.V, Berlin, 2021.

500 Englhardt, J., de Moel, H., Huyck, C. K., de Ruiter, M. C., Aerts, J. C. J. H., and Ward, P. J.: Enhancement of large-scale flood risk assessments using building-material-based vulnerability curves for an object-based approach in urban and rural areas, Nat. Hazards Earth Syst. Sci., 19, 1703–1722, 2019.

Fatemi, Md. N., Okyere, S. A., Diko, S. K., Kita, M., Shimoda, M., and Matsubara, S.: Physical Vulnerability and Local Responses to Flood Damage in Peri-Urban Areas of Dhaka, Bangladesh, Sustainability, 12, 2020.

505 Fathom: Fathom-Global 2.0 Flood Hazard Data, n.d.

Federal Emergency Management Agency (FEMA): Earthquake Model Technical Manual, HAZUS 4.2 SP3, 2020.

Fraser, S., Jongman, B., Balog, S., Simpson, A., Saito, K., and Himmelfarb, A.: The Making of a Riskier Future: How Our Decisions are Shaping Future Disaster Risk, Washington, D.C., 2016.

Gain, A. K., Mojtahed, V., Biscaro, C., Balbi, S., and Giupponi, C.: An integrated approach of flood risk assessment in the
510   eastern part of Dhaka City, Nat. Hazards, 79, 1499–1530, 2015.

Galasso, C., McCloskey, J., Pelling, M., Hope, M., Bean, C. J., Cremen, G., Guragain, R., Hancilar, U., Menoscal, J., Mwang'a,
K., Phillips, J., Rush, D., and Sinclair, H.: Editorial. Risk-based, Pro-poor Urban Design and Planning for Tomorrow's Cities,
Int. J. Disaster Risk Reduct., 58, 2021.

Gentile, R. and Galasso, C.: Simplified seismic loss assessment for optimal structural retrofit of RC buildings, Earthq. Spectra,
515   37, 346–365, 2021.

Gentile, R., Galasso, C., Jenkins, L., Manandhar, V., Menteşe, E., Guragain, R., and McCloskey, J.: Scoring, selecting, and
developing physical impact models for multi-hazard risk assessment, Int. J. Disaster Risk Reduct., 2022.

Government of Nepal, N. P. C.: Nepal Flood 2017: Post Flood Recovery Needs Assessment, Kathmandu, Nepal, 2017.

Hallegatte, S., Bangalore, M., Bonzanigo, L., Fay, M., Kane, T., and Narloch, U.: Shock Waves: Managing the Impacts of
520   Climate Change on Poverty, World Bank, Washington, DC, 2016.

Hallegatte, S., Vogt-Schilb, A., Bangalore, M., and Rozenberg, J.: Unbreakable: Building the Resilience of the Poor in the
Face of Natural Disasters, World Bank, Washington, D.C., 2017.

Hemmati, M., Ellingwood, B. R., and Mahmoud, H. N.: The Role of Urban Growth in Resilience of Communities Under Flood
Risk, Earths Future, 8, e2019EF001382, 2020.

525   Hinkel, J., Aerts, J. C. J. H., Brown, S., Jiménez, J. A., Lincke, D., Nicholls, R. J., Scussolini, P., Sanchez-Arcilla, A., Vafeidis,
A., and Addo, K. A.: The ability of societies to adapt to twenty-first-century sea-level rise, Nat. Clim. Change, 8, 570–578,
2018.

Hirabayashi, Y., Mahendran, R., Koirala, S., Konoshima, L., Yamazaki, D., Watanabe, S., Kim, H., and Kanae, S.: Global
flood risk under climate change, Nat. Clim. Change, 3, 816–821, 2013.

530   Huizinga, J., De Moel, H., and Szewczyk, W.: Global flood depth-damage functions: Methodology and the database with
guidelines, 2017.

IDMC: Global Estimates 2015: People Displaced by Disasters, Internal Displacement Monitoring Center, 2015.

Jongman, B.: Effective adaptation to rising flood risk, Nat. Commun., 9, 1986, 2018.

Jongman, B., Ward, P. J., and Aerts, J. C. J. H.: Global exposure to river and coastal flooding: Long term trends and changes,
535   Glob. Environ. Change, 22, 823–835, 2012.

Landell Mills: Nepal: Flood Risk Sector Assessment Consultant Report, Asian Development Bank, 2019.

Lasage, R., Veldkamp, T. I. E., de Moel, H., Van, T. C., Phi, H. L., Vellinga, P., and Aerts, J. C. J. H.: Assessment of the
effectiveness of flood adaptation strategies for HCMC, Nat. Hazards Earth Syst. Sci., 14, 1441–1457, 2014.

Li, W., Xu, B., and Wen, J.: Scenario-based community flood risk assessment: a case study of Taining county town, Fujian
540   province, China, Nat. Hazards, 82, 193–208, 2016.

Maqsood, S. T., Wehner, M., Ryu, H., Edwards, M., and Dale, K.: GAR15 Regional Vulnerability Functions: Reporting on the UNISDR/GA SE Asian Regional Workshop on Structural Vulnerability Models for the GAR Global Risk Assessment, 11–14 November, 2013, Geoscience Australia, Canberra, Australia, Geoscience Australia, 2014.

545 Medero, G. M., Kennedy, J. H., Woodward, P. K., and Banimahd, M.: Flooding Effect on Earth Walls, Sustainability, 3, 69–81, 2011.

Mesta, C., Cremen, G., and Galasso, C.: Quantifying the Potential Benefits of Risk-Mitigation Strategies on Present and Future Seismic Losses in Kathmandu Valley, Nepal, Earthq. Spectra, 2022a.

Mesta, C., Cremen, G., and Galasso, C.: Urban growth modelling and social vulnerability assessment for a hazardous Kathmandu Valley, Sci. Rep., 12, 6152, 2022b.

550 Ministry of Forests and Environment: Climate change scenarios for Nepal for National Adaptation Plan, Government of Nepal, Kathmandu, Nepal, 2019.

National Society for Earthquake Technology-Nepal (NSET): Final Report on Building Inventory, Damage and Seismic Intensity Survey for the JICA Aided the Project for Assessment of Earthquake Disaster Risk for the Kathmandu Valley in Nepal, Kathmandu, Nepal, 2016.

555 Nicholls, R. J., Lincke, D., Hinkel, J., Brown, S., Vafeidis, A. T., Meyssignac, B., Hanson, S. E., Merkens, J.-L., and Fang, J.: A global analysis of subsidence, relative sea-level change and coastal flood exposure, Nat. Clim. Change, 11, 338–342, 2021.

Nofal, O. M. and van de Lindt, J. W.: High-resolution flood risk approach to quantify the impact of policy change on flood losses at community-level, Int. J. Disaster Risk Reduct., 62, 102429, 2021.

Nofal, O. M., van de Lindt, J. W., and Do, T. Q.: Multi-variate and single-variable flood fragility and loss approaches for 560 buildings, Reliab. Eng. Syst. Saf., 202, 106971, 2020.

Olsen, A. S., Zhou, Q., Linde, J. J., and Arnbjerg-Nielsen, K.: Comparing Methods of Calculating Expected Annual Damage in Urban Pluvial Flood Risk Assessments, Water, 7, 2015.

Oubennaceur, K., Chokmani, K., Nastev, M., Lhissou, R., and El Alem, A.: Flood risk mapping for direct damage to residential buildings in Quebec, Canada, Int. J. Disaster Risk Reduct., 33, 44–54, 2019.

565 Rentschler, J., Salhab, M., and Jafino, B. A.: Flood exposure and poverty in 188 countries, Nat. Commun., 13, 3527, 2022.

Ruangpan, L., Vojinovic, Z., Plavšić, J., Doong, D.-J., Bahlmann, T., Alves, A., Tseng, L.-H., Randelović, A., Todorović, A., Kocic, Z., Beljinac, V., Wu, M.-H., Lo, W.-C., Perez-Lapeña, B., and Franca, M. J.: Incorporating stakeholders' preferences into a multi-criteria framework for planning large-scale Nature-Based Solutions, Ambio, 50, 1514–1531, 2021.

de Ruig, L. T., Barnard, P. L., Botzen, W. J. W., Grifman, P., Hart, J. F., de Moel, H., Sadrpour, N., and Aerts, J. C. J. H.: An 570 economic evaluation of adaptation pathways in coastal mega cities: An illustration for Los Angeles, Sci. Total Environ., 678, 647–659, 2019.

de Ruiter, M. C., de Bruijn, J. A., Englhardt, J., Daniell, J. E., de Moel, H., and Ward, P. J.: The Asynergies of Structural Disaster Risk Reduction Measures: Comparing Floods and Earthquakes, Earths Future, 9, e2020EF001531, 2021.

Sampson, C. C., Smith, A. M., Bates, P. D., Neal, J. C., Alfieri, L., and Freer, J. E.: A high-resolution global flood hazard 575 model, Water Resour. Res., 51, 7358–7381, 2015.

Scussolini, P., Tran, T. V. T., Koks, E., Diaz-Loaiza, A., Ho, P. L., and Lasage, R.: Adaptation to Sea Level Rise: A Multidisciplinary Analysis for Ho Chi Minh City, Vietnam, Water Resour. Res., 53, 10841–10857, 2017.

Smith, A., Sampson, C., and Bates, P.: Regional flood frequency analysis at the global scale, Water Resour. Res., 51, 539–553, 2015.

580 Song, J., Fu, X., Wang, R., Peng, Z.-R., and Gu, Z.: Does planned retreat matter? Investigating land use change under the impacts of flooding induced by sea level rise, Mitig. Adapt. Strateg. Glob. Change, 23, 703–733, 2018.

Suwal, R., Rodrigues, H., and Varum, H.: Structural Characterization of RC Buildings of Kathmandu Valley after Gorkha Earthquake 2015, 16th World Conference on Earthquake Engineering, Santiago, Chile, 2017.

Tate, E., Rahman, M. A., Emrich, C. T., and Sampson, C. C.: Flood exposure and social vulnerability in the United States, 585 Nat. Hazards, 106, 435–457, 2021.

Thieken, A. H., Cammerer, H., Dobler, C., Lammel, J., and Schöberl, F.: Estimating changes in flood risks and benefits of non-structural adaptation strategies - a case study from Tyrol, Austria, Mitig. Adapt. Strateg. Glob. Change, 21, 343–376, 2016.

Tiepolo, M. and Galligari, A.: Urban expansion-flood damage nexus: Evidence from the Dosso Region, Niger, Land Use 590 Policy, 108, 105547, 2021.

Timsina, N. P., Shrestha, A., Poudel, D. P., and Upadhyaya, R.: Trend of urban growth in Nepal with a focus in Kathmandu Valley: A review of processes and drivers of change, UKRI GCRF Urban Disaster Risk Hub, 2020.

United Nations, D. of E. and S. A., Population Division: World Population Prospects 2019: Highlights (ST/ESA/SER.A/423), New York, 2019a.

595 United Nations, D. of E. and S. A., Population Division: World Urbanization Prospects: The 2018 Revision (ST/ESA/SER.A/420), New York, 2019b.

Varum, H., Dumaru, R., Furtado, A., Barbosa, A. R., Gautam, D., and Rodrigues, H.: Chapter 3 - Seismic Performance of Buildings in Nepal After the Gorkha Earthquake, in: Impacts and Insights of the Gorkha Earthquake, edited by: Gautam, D. and Rodrigues, H., Elsevier, 47–63, 2018.

600 Wing, O. E. J., Lehman, W., Bates, P. D., Sampson, C. C., Quinn, N., Smith, A. M., Neal, J. C., Porter, J. R., and Kousky, C.: Inequitable patterns of US flood risk in the Anthropocene, Nat. Clim. Change, 12, 156–162, 2022.

World Meteorological Organization: WMO Atlas of Mortality and Economic Losses from Weather, Climate and Water Extremes (1970–2019), 2021.

Yamazaki, D., Ikeshima, D., Tawatari, R., Yamaguchi, T., O'Loughlin, F., Neal, J. C., Sampson, C. C., Kanae, S., and Bates, 605 P. D.: A high-accuracy map of global terrain elevations, Geophys. Res. Lett., 44, 5844–5853, 2017.

Yamazaki, D., Ikeshima, D., Sosa, J., Bates, P. D., Allen, G. H., and Pavelsky, T. M.: MERIT Hydro: A High-Resolution Global Hydrography Map Based on Latest Topography Dataset, Water Resour. Res., 55, 5053–5073, 2019.